

Radiology of Bronchiectasis



Ashkan Pakzad, MPhil^{a,b,*}, Joseph Jacob, FRCR, MD(Res)^{b,c}

KEYWORDS

- Bronchiectasis • Computed tomography • Radiology • Quantitative image analysis
- Magnetic resonance imaging

KEY POINTS

- On computed tomographic imaging, bronchiectasis appearances and distribution within the lung can suggest the underlying disease cause
- Visual scores of bronchiectasis-related damage are limited in their ability to simultaneously consider disease extent and severity
- Computer analysis of computed tomographic imaging may be a sensitive measure of disease burden and disease progression over time
- MRI of the lung can provide functional and structural information and has an important role in the evaluation of young patients and the early detection of lung damage

INTRODUCTION

Within the lungs, the airways run alongside the pulmonary arteries within the peribronchovascular interstitium, the connective tissue envelope that runs through the center of the secondary pulmonary lobule. On computed tomographic (CT) imaging, bronchi and pulmonary arteries can be seen to divide at regular intervals within the lobes. The bronchi divide at bifurcations or trifurcations with the parent airway dilating before separating into its daughter branches. Each airway division gives rise to a new airway generation, and the length of the airway between divisions is termed an airway segment. In health, the airways gradually taper or narrow in cross-sectional area as they travel toward the lung periphery.

Bronchiectasis represents the sequelae of damage to the airways and is most commonly characterized by the presence of abnormal airway dilatation and a loss of airway tapering. Bronchiectasis is

associated with a variety of lung diseases, and visual scoring systems applied to CT imaging have been used alone or in combination with clinical variables and pulmonary function tests to assess a patient's disease burden. Recent advances in computer analysis may help improve the precision and sensitivity with which disease burden and disease progression are identified on CT. Accordingly, computer tools may have an important role in evaluating drug treatment response in clinical trials as well as for real-world assessments of disease behavior.

This review describes the imaging characteristics of bronchiectasis on CT and MRI. The utility of semiquantitative visual CT scores in disease characterization is discussed. We also provide an overview of recent studies that have deployed objective computer-based quantitative image analysis in patients with bronchiectasis and describe the potential benefits and challenges related to using such tools in the coming years.

^a Departments of Medical Physics and Biomedical Engineering, and Computer Science, University College London, UK; ^b Centre for Medical Image Computing, University College London, London, UK; ^c UCL Respiratory, University College London, London, UK

* Corresponding author. UCL Engineering CMIC, 1st Floor, 90 High Holborn, London WC1V 6LJ, UK.

E-mail address: a.pakzad@cs.ucl.ac.uk

Twitter: [@AshkanPakzad](https://twitter.com/AshkanPakzad) (A.P.)

DEFINING BRONCHIECTASIS ON COMPUTED TOMOGRAPHY

Bronchiectasis was first described in the early nineteenth century by Laennec¹ in patients with tuberculosis. The existence of bronchiectasis was determined following careful auscultation of the lungs and corroboration of clinical findings with observations at postmortem examination. Today the ubiquity of volumetric CT imaging has simplified the identification of abnormal airways in the lungs. Yet the definition of bronchiectasis on CT imaging is not without its controversies. For the purposes of this review only free-standing bronchiectasis, representing airway dilatation on the background of low-attenuation lung, is considered. Traction bronchiectasis, which results from fibrosis in the lung interstitium pulling open peripheral airways, is not considered.

Pathologically bronchiectasis has been defined as “irreversible localized or diffuse bronchial dilatation, usually resulting from chronic infection, proximal airway obstruction, or congenital bronchial abnormality.”² On CT, 3 imaging features have been used to define bronchiectasis:

1. A pulmonary arterial diameter larger than the luminal diameter of the corresponding airway
2. A lack of tapering of airways as they extend toward the lung periphery
3. Visible airways within the most peripheral 1 cm of the lung

Bronchial Luminal Diameter Larger than Pulmonary Artery

Assessment of the bronchus size in relation to that of the corresponding generational pulmonary artery has been an important metric with which to determine the presence of bronchiectasis.² However, over recent years, the potential to overestimate or even underestimate the presence of bronchiectasis using this method has become apparent. It is increasingly recognized that physiologic conditions such as is seen in people living at high altitude³ and as a consequence of normal aging⁴ can result in nonpathologic airway dilatation. Spurious bronchiectasis can also be seen on CT imaging when an artery divides before its accompanying airway divides. The size of the pulmonary artery may then be compared with that of an airway of an earlier generational branch; this is particularly seen in the airways in the right middle and lingula lobes.

In pathologic states such as smoking-related lung damage or hypoxic vasoconstriction⁵ occurring in areas of chronic lung disease, the

pulmonary arteries can decrease in caliber, again giving the false impression of airway dilatation.⁶ In cases in which the airways are genuinely abnormally dilated, a suboptimal inspiratory effort during acquisition of the CT may underestimate the presence of bronchiectasis as the airways are not fully inflated. When considering all these imaging caveats, relying on an airway being enlarged relative to the adjacent artery is no longer sufficient on its own to diagnose bronchiectasis on CT imaging.

Airways Within 1 cm of the Pleural Surface

In healthy individuals, the walls of peripheral airways are thinner than the resolution limits of CT imaging. As a result the “small airways,” those with airway luminal diameters less than 2 mm, are imperceptible in health because the air lying within the airway lumen merges with the air surrounding the airway. Small airways that become bronchiectatic, however, have thickened walls and widened lumens and become visible in the lung periphery. A problem with requiring airways to be dilated in the lung periphery before diagnosing bronchiectasis occurs with diseases in which central rather than peripheral bronchiectasis predominates (Table 1).

A Lack of Airway Tapering

The most specific description of bronchiectasis on CT imaging is the “lack of tapering of bronchi”² because the airways extend from the center of the lung to the periphery (Fig. 1). Identification of a lack of normal tapering can be challenging because it requires careful scrutiny of the CT, ideally by an expert. Nontapering of airways is typically assessed over the entire length of an airway from the lobar bronchi to the most distal airways. It is also possible to compare adjacent airway segments for more focal evaluation of whether an airway is tapering appropriately.

Accessory computed tomographic signs of bronchiectasis

Accessory signs on CT that are typically associated with bronchiectasis include bronchial wall thickening and a buildup of sputum within dilated airways (see Fig. 1). In the large airways, sputum and debris can occlude the airway lumen and is manifest on CT imaging as mucous plugging. Tracing a plugged airway proximally toward the center of the lung can help distinguish a blocked airway from a pulmonary vessel, a common source of confusion. In the small airways, occlusion of the airway lumen with debris or mucus, termed an exudative bronchiolitis pattern, is manifest as tree-in-bud nodularity whereby a branching

Table 1
Lobar disease distribution on computed tomographic imaging for various causes of bronchiectasis

Cause	Lobes with Most Severe Disease	Number of Patients Considered
Idiopathic bronchiectasis	RLL and LLL ⁷	476
	Lower lobes ⁸	43
Cystic fibrosis	Upper and middle lung zones ⁹	28
	Upper lobes ¹⁰	38
	RUL, right lung ¹¹	62
Post-tuberculosis	RUL ¹²	101
	Upper lobes ¹³	42
Allergic bronchopulmonary aspergillosis	Upper lobes ¹⁴	23
	Upper lobes ¹⁵	18
Nontuberculous mycobacterial disease	LML, RML, and RUL ¹⁶	85
	Upper lobes ¹⁷	48
	RUL, RML, and LML ¹³	100
	RUL, RML, and LML ¹⁸	24
Primary ciliary dyskinesia	RML, middle, and lower lobes ¹⁹	45
	LML ²⁰	20
Postinfective/aspiration	Lower lobes ⁸	52
Immune deficiency Hypogammaglobulinemia	LLL, RLL, and RML ⁷	18

Abbreviations: LLL, left lower lobe; LML, lingula lobe; LUL, left upper lobe; RLL, right lower lobe; RML, right middle lobe; RUL, right upper lobe.

pattern of solid tubes (representing nonhollow airways) is visible.

An indirect sign of small airways disease on CT imaging is a mosaic attenuation pattern whereby lung parenchyma of decreased attenuation on inspiratory CT imaging represents air trapping (see [Fig. 1](#)) within the acini of the secondary pulmonary lobule.²¹ Expiratory CT is routinely performed today to accentuate the density differences between areas of air trapping consequent to small airways disease from normal lung, which increases in density as the air leaves the alveoli on expiration. When airway walls are thickened, comparison of the inner airway wall diameter with the pulmonary artery may result in underestimation of bronchiectasis burden.²²

The observation of at least 2 of the aforementioned 3 key imaging features of bronchiectasis, as well as accessory signs including bronchial wall thickening, mucous plugging, tree-in-bud nodularity, and small airways disease on CT, can help increase confidence when assigning a diagnosis of bronchiectasis.

CLASSIC DESCRIPTIVE APPEARANCES

Traditionally bronchiectasis has been categorized into 3 patterns on CT imaging. Cylindrical bronchiectasis is the most common form and as its name

implies, demonstrates smooth dilatation throughout the length of the airway. Varicose bronchiectasis demonstrates a ruffled, beaded contour to the airway and is typically seen in association with allergic bronchopulmonary aspergillosis (ABPA) infection and in posttuberculous airway damage. Cystic bronchiectasis where an airway is dilated into a rounded sphere is typically seen associated with cystic fibrosis (CF) and following tuberculous infection.

The location of bronchiectasis can also provide a clue as to the underlying disease cause. Central bronchiectasis is more commonly seen in ABPA, CF, and congenital tracheobronchomegaly (Mounier Kuhn syndrome). For peripheral bronchiectasis, the lobar distribution of disease can provide clues to the cause (see [Table 1](#)).

CLINICAL COMPUTED TOMOGRAPHIC EVALUATION

The optimal CT acquisition for the evaluation of bronchiectasis is a volumetric scan in which CT slices are a maximum of 1 mm in thickness in the axial plane. Evaluation of sagittal and coronal image reconstructions can aid in the delineation of airway dilatation and any lack of airway tapering. When performing longitudinal CT imaging in a patient, it is essential to have each CT time point

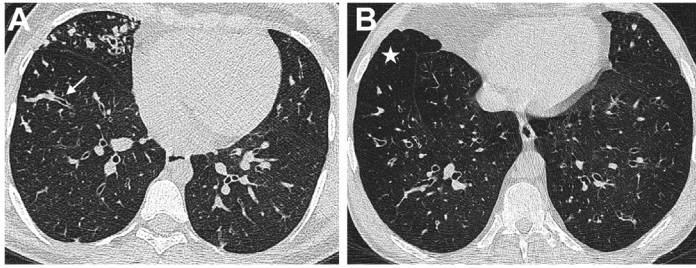


Fig. 1. Axial CT images demonstrating (A) free-standing bronchiectasis and mucous-filled airways (arrow) and (B) functional small airways disease (star).

imaged using the same CT scanner and reconstruction kernels to keep scanner-related measurement noise to a minimum.

Although considerable effort has gone into understanding the measurement variability associated with pulmonary function tests, understanding CT-related measurement variability remains a nascent field. Yet understanding what degree of change in longitudinal CT measurements reflects genuine disease deterioration as opposed to change resulting from measurement variation is essential to the development of robust prognostic tools. In addition to scanner-related measurement variability, differing patient effort between time points can strongly impact the assessment of bronchiectasis severity. For the follow-up of a patient with bronchiectasis, CTs are not typically performed at regular time intervals according to standardized protocols. Instead, a repeat CT is usually requested when a patient has clinically deteriorated, often with accompanied breathlessness. An unintended consequence is that a CT performed at the time of an exacerbation of disease will often be of inferior quality compared with a CT acquired when the patient was clinically well. The repeat CT may provide valuable information such as the presence of infection but will be compromised in its ability to describe the natural history or trajectory of the underlying disease.

When evaluating lung damage related to bronchiectasis, several visual scoring methods have been used. These scores typically assess a variety of imaging patterns (Table 2) using categorical scales on a lobar basis. One important limitation when using these semiquantitative visual scores relates to their consideration of bronchiectasis extent and severity as 2 variables that compete in prognostic models. Yet separating the impact of bronchiectasis extent from bronchiectasis severity seems rather simplistic. Visual analyses ask to choose whether subtle dilatation of the airways in 3 bronchopulmonary segments of the lower lobes (extensive disease) is more prognostically important than marked dilatation of an airway (severe bronchiectasis) in a single bronchopulmonary segment. There is no easy reproducible way for visual CT scores to simultaneously consider

both bronchiectasis extent and severity, but this is an area in which the application of computational analyses to CT imaging could add real value.

Detailed semiquantitative visual CT scores including the Brody^{20,33,34} and Bhalla^{35,36} scores are often performed by specialists. These lobar scores are time consuming and may demonstrate variable interobserver agreement.³⁷ As a result, their clinical utility in the real-world evaluation of patient disease burden is limited. Yet such scores can delineate unique imaging phenotypes of bronchiectasis.³⁸ The assessment of disease progression on longitudinal CT imaging can be challenging when using visual scores because some areas of a CT might appear improved (with reduced mucous plugging or tree-in-bud opacification), yet with disease having worsened in other regions (Fig. 2). Visual scores of disease evolution on longitudinal CTs are typically analyzed on a whole-lung level, with the result that localized changes in disease extent/severity are often lost. Developing robust methods with which to evaluate bronchiectasis-related disease progression using visual CT scores remains an open challenge.

An alternative to complex visual scoring systems lies with the use of multidimensional bronchiectasis disease scores, which take clinical, imaging, and functional measurements to estimate disease burden. Such scores often only consider limited numbers of imaging variables and are therefore easier to perform. CT variables used in multidimensional bronchiectasis scores include bronchiectasis extent used in the FACED score (forced expiratory volume in 1 second [FEV₁], age, chronic colonization, extension, and dyspnea)^{12,39,40} or in the Bronchiectasis Severity Index: bronchiectasis extent or the presence of cystic bronchiectasis.^{41,42} The Bronchiectasis Radiologically Indexed CT Score considers bronchiectasis severity and the number of bronchopulmonary segments containing emphysema.

COMPUTER ANALYSIS OF BRONCHIECTASIS

Over the past 10 years, rapid advances in the processing power of computers have resulted in the

Table 2
Variables analyzed using semiquantitative visual analysis of computed tomographic imaging

CT Variable	0	1	2	3
Severity of bronchiectasis	Absent	Mild: luminal diameter slightly greater than vessel diameter	Moderate: luminal diameter 2–3 times greater than vessel diameter	Severe: luminal diameter >3 times greater than vessel diameter
Extension of bronchiectasis (number of affected segments)	Absent	1–5	6–9	>9
Bronchial wall thickening	Absent	Mild: wall thickness = vessel diameter	Moderate: wall thickness 2 times the vessel diameter	Severe: wall thickness >2 times the vessel diameter
Mucous plugging (number of affected segments)	Absent	1–5	6–9	>9
Sacculations (number of affected segments)	Absent	1–5	6–9	>9
Involvement of bronchial generations	Absent	>4th generation	>5th generation	>6th generation
Bullae	Absent	Unilateral (<4)	Bilateral (<4)	>4
Air trapping (low attenuation) (number of affected segments)	Absent	1–5	>5	
Atelectasis	Absent	Subsegmental	Segmental/lobar	
Emphysema (number of affected segments)	None	1–5	>5	
Consolidation/collapse	None	Subsegmental	Segmental/lobar	

development of the field of quantitative medical image analysis. The aim has been to use computers to identify structures in organs such as the lung at a voxel level. By measuring the number of voxels and the location of structures within the lung, it should be possible to provide precise objective measurements that reflect healthy and diseased tissue. The earliest and simplest methods used Hounsfield unit (HU) density thresholds to categorize tissue as emphysema.⁴³

With regard to evaluating bronchiectasis, the key challenge has been computational delineation and measurement of the airways in the lung. In theory identifying all the voxels that constitute airways on a CT could provide a detailed volume of the airways. Expressing this as a percentage of total lung volume would normalize the airway measurement for an individual and remove the influence of differences in patient size or gender. By measuring the difference in inner and outer

airway wall diameters it would also be possible to derive an estimate of airway wall thickening.

Yet computational analysis of the airways is a challenging task; it primarily involves 2 processes. First, the lumen of the airways needs to be identified, a process termed segmentation. The second stage incorporates the specific calculations used to characterize or quantify airway features that indicate damage, all of which rely on the airway segmentation.

Several factors can affect the ability to segment the airways on a CT.⁴⁴ Inherent quantum noise is present on a CT and is influenced by factors including radiation dose, detector size, and patient size. Quantum noise is responsible for the graininess of CT images and is noticeably greater on low-dose CT acquisitions. The reconstruction algorithm used for a CT acquisition has a major impact on image interpretation by computer algorithms. The axial plane slice thickness of a CT

Table 3
Studies that have deployed quantitative analysis of computed tomographic imaging in patients with bronchiectasis over the last 10 years

Study	Quantitative Method	Cohort Studied	Study Patient Number	Age (Years, Range)	Findings
Wielpütz et al. ²⁵ 2013	Outer airway diameter, wall thickness, lumen area of segmented airways	Adults with CF and healthy adults Children with CF and healthy children	37	4–68	Outer airway diameter and wall thickness both larger in patients with CF than in controls. Significant correlations between all quantitative measures and FEV ₁ in adults
DeBoer et al. ²² 2014	Count of identifiable airways on inspiratory CT slices. Air trapping percentage on expiratory slices	Children with CF compared with normal controls	35	6–15	Average airway count per slice and air trapping percentage higher in patients with CF than in controls. Average peripheral airway count correlated with visual CT scores and lung function (FEV ₁ and FVC). Air trapping percentage correlated with visual CT scores
Santos et al. ²³ 2016	Number of airway segments, airway lumen size, and wall thickness	Patients with CF split using baseline FEV ₁ %	34	7–43	Greater number of airway segments in the higher FEV ₁ group. Significant correlations in wall thickness ratio for third- to eighth-generation airways with FEV ₁ . Correlations stronger in lower FEV ₁ group.

Kuo et al. ²⁶ 2017	Luminal AA ratio, outer wall AA ratio, wall thickness-artery ratio for identifiable AA pairs	Children with CF compared with normal subjects at baseline and 2 y	12	0.6–5.2	Outer AA ratio and wall thickness-artery ratios significantly different between CF and controls at both time points. Inner and outer AA ratio significantly increased longitudinally in CF
Kuo et al. ²² 2017	Lumen AA ratio, outer AA ratio, airway wall thickness for all identifiable AA pairs	Adolescents with CF compared with normal controls	11	8.7–15.0 (IQR)	Outer AA ratio and airway wall thickness showed significant differences between subjects with CF and normal subjects independent of lung volume. Differences increased at each distal segmental generation
Diaz et al. ⁶ 2017	Airway and artery lumen size, luminal AA ratio, PWA, wall thickness, wall area percentage for fourth- to sixth-generation airways	Compared smokers with BE with normal subjects	21	67.0 ± 9.5 (mean ± SD)	Inner AA ratio, wall thickness, wall area percentage greater in BE than controls. No difference in airway lumen, but artery diameters smaller in BE than controls
Diaz et al. 2018 ²⁷	Lung blood vessel volume	Smokers with and without BE	155	45–80	Patients with BE had more vascular pruning in the distal lung. Those with vascular pruning had lower FEV ₁

(continued on next page)

Table 3
(continued)

Study	Quantitative Method	Cohort Studied	Study Patient Number	Age (Years, Range)	Findings
Bak et al. ²⁸ 2018	Air trapping percent calculated using mean I/E lung density ratio	Different levels of severity of BE in COPD patients.	73	48–96	Patients with COPD with BE showed significantly higher severe lung density ratio than patients with COPD without BE. Lung density ratio correlated with BE severity
Hoang-Thi, ²⁹ 2018	Fixed and adapted CT density threshold scores in PCD	Correlate automated lung density with lung function tests	62	39 ± 15 (mean ± SD)	Mean lung density plus 1 SD correlated better with FEV ₁ and FVC than visual CT scores
Kuo et al. ³⁰ 2020	Tapering of airways and outer wall AA ratio	Children with CF compared with controls groups	12	5.5–15.0 (IQR)	Significantly reduced airway tapering seen across all airways. Increased outer AA ratio in small airways compared with control groups
Robinson et al. ³¹ 2020	Air trapping percentage	Children with CF followed up at 3 mo and 1 and 2 y	36	7.3–17.5	Quantitative air trapping and visual CT mucous plugging scores increased at 1- and 2-y follow up
Xing et al. ³² 2020	CT features with machine learning	Differentiate between NTM and PTB using 103 CT-derived features	116	30–76	Shape and tissue texture features that represented bronchiectasis were found to be the best discriminators of NTM and PTB

Abbreviations: AA, airway-artery; BE, bronchiectasis; CF, cystic fibrosis; COPD, chronic obstructive pulmonary disease; FEV₁, forced expiratory volume in 1 s; FVC, forced vital capacity; I/E, inspiratory-expiratory; IQR, interquartile range; NTM, nontuberculous mycobacteria; PCD, primary ciliary dyskinesia; PTB, pulmonary tuberculosis; PWA, peak wall attenuation; SD, standard deviation.

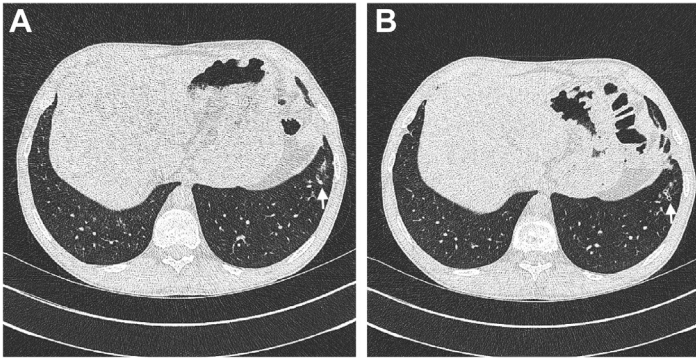


Fig. 2. Progressive dilatation of peripheral airways (*arrow*) seen in axial CT images *A* and *B* captured 12 months apart in a patient with nontuberculous mycobacterial infection. The extent of bronchiectasis as well as the severity of dilatation had increased in the lungs over time, but visual CT scores consider extent and severity of disease separately.

image influences the spatial resolution of the image and ideally should be less than 1.5 mm. Modern iterative reconstruction algorithms have been designed with the aim of lower radiation dose aimed to denoise the image but can appear different to a computer when compared with images acquired using traditional filtered back projection techniques. High-resolution reconstruction algorithms enhance image contrast or use edge enhancement of linear structures, which help visual interpretation of structures in the lung, but can confound computational image interpretation. There has been a call for standardized computer-friendly reconstruction kernels to be available on all CT machines, which would aid image interpretation by computers and allow robust comparisons across time points. Yet with many reconstruction algorithms remaining propriety to commercial scanner manufacturers, this goal is yet to be realized.

Other constraints to computer analysis of CTs are common to visual CT analysis, and include breathing artifacts on the image, intercurrent infection limiting the number of airways that are visible, the quality of inspiration by the patient at the time of the scan, and the consistency of image acquisition across CT time points.

QUANTITATIVE COMPUTED TOMOGRAPHIC ANALYSIS

Quantitative CT metrics typically reflect 1 of 3 analytical approaches:

1. A representation of real physical properties, such as airway diameter, typically considered in visual CT scores.
2. Texture analysis in which small regions/patches of the CT are classified by appearance, with descriptions of the patterns terms based on radiological terms.

3. Latent features that often do not have an easily interpretable visual equivalent.

Quantitative metrics that have been applied to evaluate bronchiectasis (**Table 3**) are the following

Number of Resolvable Airways

As described earlier, as bronchiectasis worsens, more airway segments become visible on the CT. Quantifying the number of visible airway segments on a CT, a task that could be rapidly performed by computational tools, could therefore be a powerful indicator of disease extent. Sampling of airway counts on interspaced CT imaging has been performed in patients with CF.²⁴ With volumetric imaging, more precise airway counts can be computed by calculating the number of airway segments between airway branching points using an airway segmentation.^{22,25} Yet this method is heavily reliant on the particular CT acquisition protocol and reconstruction kernels used.

Airway Measurements

The most commonly used airway measurements consider either airway diameters or cross-sectional areas, with the measurement being acquired in a plane perpendicular to the airway's central axis.⁴⁵ Although the inner airway wall diameter is often visually compared with the pulmonary artery to detect bronchiectasis, airway wall inflammation can make an airway lumen size appear much smaller than it really is, disguising the presence of bronchiectasis. As a result, measurement of the airway diameter/cross-sectional area using the outer airway wall is more typically used with computational analysis. Several studies in CF and smokers with radiological bronchiectasis have shown that the airway lumen size is no different to that of that of control populations. However when airways are measured using the outer airway wall, both airway size and wall

thickness have been shown to be significantly different in disease populations compared with healthy subjects.^{6,23,25}

Tapering of an airway can be identified using computational analysis by measuring cross-sectional areas or diameters of airways at regular intervals along the airway centerline.⁴⁵ A challenge lies in the transient dilatation seen at airway bifurcations that could suggest artifactual bronchiectasis. The only study to have considered tapering metrics demonstrated reduced airway tapering in pediatric patients with CF when compared with healthy participants when using both inner and outer airway wall measurements.³⁰ Tapering metrics may work well in the assessment of cylindrical bronchiectasis, where dilatation is relatively constant through the length of the airway. However, tapering measurement of varicose and cystic bronchiectasis in which dilatation and narrowing can coexist in a single airway might be more challenging.

Air Trapping

Airway inflammation with narrowing and loss of compliance can result in air trapping within the acinus. Although the blocked airway may not be resolvable on CT, its sequelae of dilated secondary pulmonary lobules is visible on inspiratory CTs and accentuated on expiratory scans. Air trapping can therefore be quantified at a voxel level. Simple methods to quantify air trapping have utilized HU density thresholds (-850 HU) on expiratory CTs.^{24,31} The parametric response map method compares HU threshold changes across registered inspiratory and expiratory CTs to classify emphysema and functional small airways disease. On the inspiratory CT, all voxels of less than -950 HU are considered to represent emphysema. Following registration of the expiratory CT to the inspiratory CT, any nonemphysematous voxels with a HU density <-856 on the expiratory CT are considered regions of functional small airways disease. Varying HU density thresholds have been used to categorize the severity of air trapping.⁴⁶ Yet a requirement of all these methods is an adequate-quality inspiratory and expiratory CT acquisition. A way of optimizing breath holds lies in real-time spirometric feedback to the patient during the CT acquisition so that they are aware when they should breathe in and breathe out.²⁹

Airway-Artery Ratio

Challenges in delineating bronchiectasis using visual evaluation of the airway-artery ratio have already been described. Yet quantitative measurements of the airway-artery ratio have demonstrated significant correlations with CF disease severity in adolescent

patients.^{22,23,43} In adult smokers diagnosed with radiological bronchiectasis, however, in whom the airway-artery ratio was found to be greater than in control subjects, it was shown that rather than differences in airway size between groups, it was the artery that was smaller in patients compared with the control group.⁶

Other Quantitative Computed Tomographic Measures

There are several quantification measures that have not been as frequently reported in the context of bronchiectasis.

Although artery size has been frequently analyzed, the general quantification of vessel volume has rarely been reported in studies of patients with bronchiectasis. A reduction in the volume of small vessels (<5 mm² in cross section) in the peripheral lung,²⁷ termed vascular pruning, has been shown to occur in smokers with mild radiological bronchiectasis. In smokers with bronchiectasis, the presence of peripheral vascular pruning was associated with reduced 6-minute walk test distances and FEV₁.

Using methods analogous to characterizing air trapping with CT density thresholds, automated CT density analysis has been used to group different HU values within the lung into several distinct thresholds. The thresholds can be fixed or adaptive based on the HU histogram for the whole-lung CT range to account for individual variation in inspiration. A study in adults with CF using such an approach showed that density thresholds correlated better with longitudinal disease severity than visual CT scores.⁴⁶ Another study using adaptive thresholds in patients with primary ciliary dyskinesia demonstrated density thresholds correlating better with disease severity measures (FEV₁ and forced vital capacity) at baseline than visual CT scores.²⁹

Xing and colleagues, in 2020, considered 103 computer-derived CT variables, each of which represented a different latent CT feature.³² Shapes and tissue features that represented bronchiectasis were shown to be the best discriminators for differentiating nontuberculous mycobacterial infection from pulmonary tuberculosis infection.

CHALLENGES IN BRONCHIECTASIS QUANTIFICATION

Most quantitative studies considered in this review were performed in patients with CF. The relative abundance of imaging data in CF makes it an easier disease process to study and develop automated tools. Should the computer-based tools developed in CF populations be transferred to

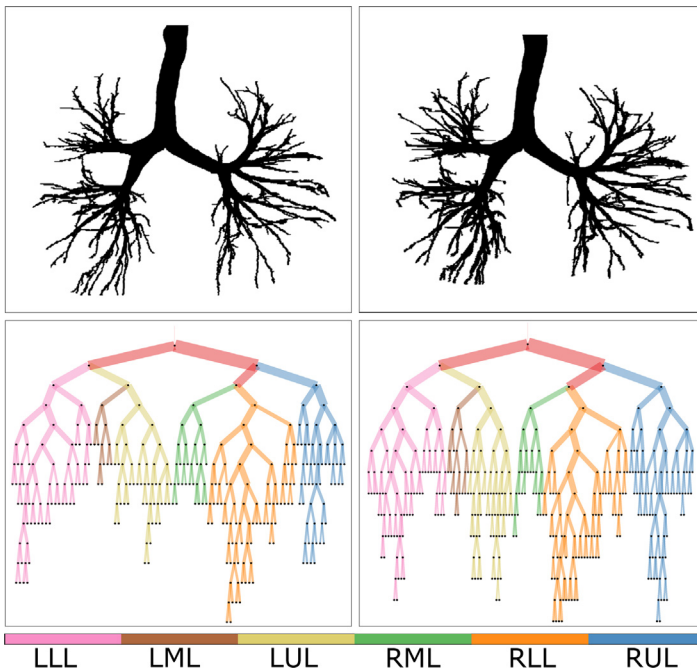


Fig. 3. Airway segmentations of a patient with bronchiectasis (*top row*) derived from 2 chest computed tomographic scans taken 8 months apart. Airway graph networks of the airways in the lung (*bottom row*), where the airway segments are represented as branches. Branch thickness is proportionate to the average airway diameter computed by automated quantification of the computed tomographic image. The separate lobes have been labeled by color. The lingula has been considered as a separate lobe. LLL, left lower lobe; LML, lingula lobe; LUL, left upper lobe; RML, right middle lobe; RLL, right lower lobe; RUL, right upper lobe.

analyze non-CF populations they will need to be fine-tuned and optimized to learn the unique imaging characteristics of the new bronchiectasis disease populations. Optimizing computer algorithms ideally requires large datasets of cases wherein the imaging parameters and variety of patients included are diverse enough to ensure that there is no bias in the training data.

The performance of computer algorithms is heavily influenced by the training data used to develop the algorithm. Should the training data not have sufficient representation of patients of different ages, or consider gender, ethnic, socioeconomic, or geographic distribution of cases adequately, there is a risk of introducing bias into the computer model. To have a computer algorithm that is robust in performance and generalizable to new datasets, it should be trained on large diverse datasets. In this regard collaboratives such as Bronch-UK⁴⁷ and EMBARC⁴⁸ will be valuable resources for the development of bronchiectasis-specific computer algorithms.

Regarding newer deep learning computer methods, an algorithm may identify a patient as likely to have a poor clinical outcome, but it may not be able to demonstrate in visual terms what features on the CT are driving the decision that the outcome will be poor. The need to be able to see what a computer model is basing its prognostic prediction on is important to gain clinician and patient trust that the right decision is being

made by the computer. Being able to interpret computer-derived imaging features can help ascribe a biological explanation as to why the imaging features link to reduced survival, which in turn can help in the delineation of disease pathophysiology and drug development.

It is clear that visual CT evaluation is sufficient for disease detection. The real advantage of computer analysis of CT imaging is likely to be in longitudinal analysis of disease severity and extent change (**Fig. 3**). The development of quantitative CT metrics is likely to increasingly focus on measuring longitudinal disease progression, which a human observer cannot quantify with the same precision. To train such models adequately, large diverse longitudinal datasets will be imperative. The algorithms will also need to focus on improving automated airway segmentations to identify as many abnormal peripheral airways as possible and be able to detect and quantify mucous plugging in airways, a task for which deep learning may be well suited.^{32,49}

QUANTITATIVE MRI ANALYSIS

As well as having a higher inherent signal-to-noise ratio, CT imaging has a much faster image acquisition time than MRI. A rapid image acquisition avoids motion artifacts because the whole CT study can be performed within a single breath hold. The greater spatial resolution with CT also

allows the resolution of larger numbers of smaller airway branches. The main constraint with CT imaging is the exposure of patients to ionizing radiation. In young populations undergoing repeated imaging such as patients with CF or primary ciliary dyskinesia this can result in a cumulative increased risk of developing cancer. MRI is therefore being increasingly used for the assessment of younger patients with airways disease and has the added advantage of providing insights into the functional impact of lung disease.

Studies utilizing quantitative MRI focus primarily on lung ventilatory defects. Differences in non-contrast-enhanced magnetic resonance (MR) signal intensity between inspiratory and expiratory MR scans has been found to correlate with lung function measures in patients with CF.⁴⁴ The inhalation of inert hyperpolarized noble gases such as ³He during MRI acquisition has been shown to accentuate the MR spin magnetization of the noble gas, which increases the MR signal-to-noise ratio within the lungs. When the hyperpolarized gas diffuses into the airspaces, it is possible to get a measure of lung ventilation by calculating the volume of lung that has a low ³He MR signal. In patients with bronchiectasis, quantification of ventilatory defects has been shown to be increased in lobes showing bronchiectasis on CT, and in lobes with no bronchiectasis on CT when compared with healthy subjects.⁵⁰ Ventilatory improvements have also been demonstrated following airway clearance therapy in patients with non-CF bronchiectasis.⁵¹ Detecting ventilatory defects using hyperpolarized gas MRI is likely to be a sensitive method by which to detect early lung damage, particularly in young patients, thereby avoiding radiation exposure.⁵⁰

SUMMARY

Bronchiectasis on CT imaging is best identified by considering together a lack of airway tapering, enlargement of an airway relative to its accompanying pulmonary artery, and evidence of enlarged airways in the lung periphery. Bronchiectasis patterns and distribution on visual CT evaluation can point to underlying disease causes. MR analysis of bronchiectasis is a rapidly advancing field that provides functional as well as structural information on lung disease and will play a key role in assessment of younger patients and patients with early disease.

When characterizing lung damage on CT imaging and particularly disease progression over time, visual scores are time consuming and do not easily consider disease extent and severity together. It is likely that automated computer tools

will replace visual analysis in the coming years, particularly when evaluating disease progression. For computer tools to perform at their best, training data need to be diverse and large, thereby minimizing inherent biases in the dataset. Bronchiectasis registries are likely to be an important resource to allow training of specific computer tools that may perform better than tools that have been trained on CF datasets but repurposed for bronchiectasis assessment. The easy deployment of such algorithms in hospital settings will be crucial to prevent computer tools from being instruments only used in research studies.

CLINICAL CARE POINTS

- Visual CT assessment is necessary for the diagnosis of bronchiectasis.
- Bronchiectasis can be identified by non-tapering of an airway on CT.
- Visualisation of an airway within the outer 1cm of the lung parenchyma also indicates the presence of bronchiectasis.
- A bronchiole may appear larger than its accompanying pulmonary artery for reasons unrelated to airways disease. The pulmonary artery:airway ratio is therefore not an optimal way of assessing for the presence of bronchiectasis.

DISCLOSURE

A. Pakzad is funded jointly by the Cystic Fibrosis Trust and EPSRC i4health, centre for doctoral training studentship. J. Jacob reports fees from Boehringer Ingelheim, Roche, NHSX, and GlaxoSmithKline unrelated to the submitted work. J. Jacob was supported by Wellcome Trust Clinical Research Career Development Fellowship 209553/Z/17/Z and the NIHR UCLH Biomedical Research Centre, UK.

REFERENCES

1. Laennec RT. *De l'auscultation Médiante: Ou Traité Du Diagnostic Des Maladies Des Poumons et Du Coeur*, vol. 2. Brossier; 1819.
2. Hansell DM, Bankier AA, MacMahon H, et al. Fleischner society: glossary of terms for Thoracic imaging. *Radiology* 2008;246(3):697–722. <https://doi.org/10.1148/radiol.2462070712>.
3. Kim JS, Müller NL, Park CS, et al. Bronchoarterial ratio on thin section CT: comparison between high altitude and sea level. *J Comput Assist Tomogr* 1997; 21(2):306–11.

4. Matsuoka S, Uchiyama K, Shima H, et al. Bronchoarterial ratio and bronchial wall thickness on high-resolution CT in asymptomatic subjects: correlation with age and smoking. *AJR Am J Roentgenol* 2003;180(2):513–8. <https://doi.org/10.2214/ajr.180.2.1800513>.
5. Dunham-Snary KJ, Wu D, Sykes EA, et al. Hypoxic pulmonary vasoconstriction: from molecular mechanisms to medicine. *Chest* 2017;151(1):181–92. <https://doi.org/10.1016/j.chest.2016.09.001>.
6. Diaz AA, Young TP, Maselli DJ, et al. Quantitative CT measures of bronchiectasis in smokers. *Chest* 2017;151(6):1255–62. <https://doi.org/10.1016/j.chest.2016.11.024>.
7. Ridge CA, Bankier AA, Eisenberg RL. Mosaic attenuation. *AJR Am J Roentgenol* 2011;197(6):W970–7. <https://doi.org/10.2214/AJR.11.7067>.
8. Kuo W, de Bruijne M, Petersen J, et al. Diagnosis of bronchiectasis and airway wall thickening in children with cystic fibrosis: objective airway-artery quantification. *Eur Radiol* 2017;27(11):4680–9. <https://doi.org/10.1007/s00330-017-4819-7>.
9. Brody AS, Kosorok MR, Li Z, et al. Reproducibility of a scoring system for computed tomography scanning in cystic fibrosis. *J Thorac Imaging* 2006;21(1):14–21. <https://doi.org/10.1097/01.rti.0000203937.82276.ce>.
10. Santamaria F, Montella S, Tiddens HAWM, et al. Structural and functional lung disease in primary ciliary dyskinesia. *Chest* 2008;134(2):351–7. <https://doi.org/10.1378/chest.07-2812>.
11. Goeminne PC, Soens J, Scheers H, et al. Effect of macrolide on lung function and computed tomography (ct) score in non-cystic fibrosis bronchiectasis. *Acta Clin Belg* 2012;67(5):338–46. <https://doi.org/10.2143/ACB.67.5.2062687>.
12. Bhalla M, Turcios N, Aponte V, et al. Cystic fibrosis: scoring system with thin-section CT. *Radiology* 1991;179(3):783–8. <https://doi.org/10.1148/radiology.179.3.2027992>.
13. Diab-Cáceres L, Girón-Moreno RM, García-Castillo E, et al. Predictive value of the modified Bhalla score for assessment of pulmonary exacerbations in adults with cystic fibrosis. *Eur Radiol* 2021;31(1):112–20. <https://doi.org/10.1007/s00330-020-07095-y>.
14. de Brito MCB, Ota MK, Leitão Filho FSS, et al. Radiologist agreement on the quantification of bronchiectasis by high-resolution computed tomography. *Radiol Bras* 2017;50(1):26–31. <https://doi.org/10.1590/0100-3984.2015.0146>.
15. Cowman SA, Jacob J, Obaidee S, et al. Latent class analysis to define radiological subgroups in pulmonary nontuberculous mycobacterial disease. *BMC Pulm Med* 2018;18(1):145. <https://doi.org/10.1186/s12890-018-0675-8>.
16. Martínez-García MÁ, Gracia J, Relat MV, et al. Multidimensional approach to non-cystic fibrosis bronchiectasis: the FACED score. *Eur Respir J* 2014;43(5):1357–67. <https://doi.org/10.1183/09031936.00026313>.
17. Martínez-García M, Athanazio R, Girón R, et al. Predicting high risk of exacerbations in bronchiectasis: the E-FACED score. *Int J Chron Obstruct Pulmon Dis* 2017;12:275–84. <https://doi.org/10.2147/COPD.S121943>.
18. Wang H, Ji X-B, Li C-W, et al. Clinical characteristics and validation of bronchiectasis severity score systems for post-tuberculosis bronchiectasis. *Clin Respir J* 2018;12(8):2346–53. <https://doi.org/10.1111/crj.12911>.
19. Chalmers JD, Goeminne P, Aliberti S, et al. The bronchiectasis severity Index. An international derivation and validation study. *Am J Respir Crit Care Med* 2013;189(5):576–85. <https://doi.org/10.1164/rccm.201309-1575OC>.
20. McDonnell MJ, Aliberti S, Goeminne PC, et al. Multidimensional severity assessment in bronchiectasis: an analysis of seven European cohorts. *Thorax* 2016;71(12):1110–8. <https://doi.org/10.1136/thoraxjnl-2016-208481>.
21. Gevenois PA, De Vuyst P, Sy M, et al. Pulmonary emphysema: quantitative CT during expiration. *Radiology* 1996;199(3):825–9. <https://doi.org/10.1148/radiology.199.3.8638012>.
22. DeBoer EM, Swiercz W, Heltshe SL, et al. Automated ct scan scores of bronchiectasis and air trapping in cystic fibrosis. *Chest* 2014;145(3):593–603. <https://doi.org/10.1378/chest.13-0588>.
23. Santos MK, Cruvinel DL, Menezes MB, et al. Quantitative computed tomography analysis of the airways in patients with cystic fibrosis using automated software: correlation with spirometry in the evaluation of severity. *Radiol Bras* 2016;49(6):351–7. <https://doi.org/10.1590/0100-3984.2015.0145>.
24. Quan K, Shipley RJ, Tanno R, et al. Tapering analysis of airways with bronchiectasis. In: Angelini ED, Landman BA, editors. *Medical imaging 2018: image processing*, Vol. 10574. SPIE; 2018. p. 87. <https://doi.org/10.1117/12.2292306>.
25. Wielpütz MO, Eichinger M, Weinheimer O, et al. Automatic airway analysis on multidetector computed tomography in cystic fibrosis: correlation with pulmonary function testing. *J Thorac Imaging* 2013;28(2):104–13. <https://doi.org/10.1097/RTI.0b013e3182765785>.
26. Kuo W, Perez-Rovira A, Tiddens H, et al. Airway tapering: an objective image biomarker for bronchiectasis. *Eur Radiol* 2020;30(5):2703–11. <https://doi.org/10.1007/s00330-019-06606-w>.
27. Robinson TE, Goris ML, Moss RB, et al. Mucus plugging, air trapping, and bronchiectasis are important outcome measures in assessing progressive childhood cystic fibrosis lung disease. *Pediatr Pulmonol* 2020;55(4):929–38. <https://doi.org/10.1002/ppul.24646>.
28. Diaz AA, Maselli DJ, Rahaghi F, et al. Pulmonary vascular pruning in smokers with bronchiectasis. *ERJ Open Res* 2018;4(4). <https://doi.org/10.1183/23120541.00044-2018>.

29. Chassagnon G, Martin C, Burgel P-R, et al. An automated computed tomography score for the cystic fibrosis lung. *Eur Radiol* 2018;28(12):5111–20. <https://doi.org/10.1007/s00330-018-5516-x>.
30. Hoang-Thi T-N, Revel M-P, Burgel P-R, et al. Automated computed tomographic scoring of lung disease in adults with primary ciliary dyskinesia. *BMC Pulm Med* 2018; 18(1):194. <https://doi.org/10.1186/s12890-018-0758-6>.
31. Xing Z, Ding W, Zhang S, et al. Machine learning-based differentiation of nontuberculous mycobacteria lung disease and pulmonary tuberculosis using CT images. *Biomed Res Int* 2020;e6287545. <https://doi.org/10.1155/2020/6287545>.
32. BRONCH-UK. The UK bronchiectasis network and biobank. Available at: <https://www.bronch.ac.uk/>. Accessed April 15, 2021.
33. EMBARC the European bronchiectasis registry. Available at: <https://www.bronchiectasis.eu/>. Accessed April 15, 2021.
34. Nardelli P, Lanng MB, Møller CB, et al. Accurate measurement of airway morphology on chest CT images. In: *Image analysis for moving organ, breast, and thoracic images*. Springer International Publishing; 2018. p. 335–47. https://doi.org/10.1007/978-3-030-00946-5_34.
35. Pennati F, Borzani I, Moroni L, et al. Longitudinal assessment of patients with cystic fibrosis lung disease with multivolume noncontrast MRI and spirometry. *J Magn Reson Imaging* 2020. <https://doi.org/10.1002/jmri.27461>.
36. Marshall H, Horsley A, Taylor CJ, et al. Detection of early subclinical lung disease in children with cystic fibrosis by lung ventilation imaging with hyperpolarised gas MRI. *Thorax* 2017;72(8):760–2. <https://doi.org/10.1136/thoraxjnl-2016-208948>.
37. Svenningsen S, Guo F, McCormack DG, et al. Non-cystic fibrosis bronchiectasis: regional abnormalities and response to airway clearance therapy using pulmonary functional magnetic resonance imaging. *Acad Radiol* 2017;24(1):4–12. <https://doi.org/10.1016/j.acra.2016.08.021>.
38. Qi Q, Wang W, Li T, et al. Aetiology and clinical characteristics of patients with bronchiectasis in a Chinese Han population: a prospective study. *Respirology* 2015;20(6):917–24. <https://doi.org/10.1111/resp.12574>.
39. Shoemark A, Ozerovitch L, Wilson R. Aetiology in adult patients with bronchiectasis. *Respir Med* 2007;101(6): 1163–70. <https://doi.org/10.1016/j.rmed.2006.11.008>.
40. Nathanson I, Conboy K, Murphy S, et al. Ultrafast computerized tomography of the chest in cystic fibrosis: a new scoring system. *Pediatr Pulmonol* 1991;11(1): 81–6. <https://doi.org/10.1002/ppul.1950110112>.
41. Santis G, Hodson ME, Strickland B. High resolution computed tomography in adult cystic fibrosis patients with mild lung disease. *Clin Radiol* 1991;44(1):20–2. [https://doi.org/10.1016/S0009-9260\(05\)80220-X](https://doi.org/10.1016/S0009-9260(05)80220-X).
42. Mott LS, Park J, Gangell CL, et al. Distribution of early structural lung changes due to cystic fibrosis detected with chest computed tomography. *J Pediatr* 2013;163(1):243–8.e3. <https://doi.org/10.1016/j.jpeds.2012.12.042>.
43. Miura K, Nakamura M, Taooka Y, et al. Comparison of the chest computed tomography findings between patients with pulmonary tuberculosis and those with Mycobacterium avium complex lung disease. *Respir Investig* 2020;58(3):137–43. <https://doi.org/10.1016/j.resinv.2019.12.006>.
44. Panchal N, Bhagat R, Pant C, et al. Allergic bronchopulmonary aspergillosis: the spectrum of computed tomography appearances. *Respir Med* 1997;91(4):213–9. [https://doi.org/10.1016/S0954-6111\(97\)90041-X](https://doi.org/10.1016/S0954-6111(97)90041-X).
45. Mitchell TAM, Hamilos DL, Lynch DA, et al. Distribution and severity of bronchiectasis in allergic bronchopulmonary aspergillosis (ABPA). *J Asthma* 2000;37(1): 65–72. <https://doi.org/10.3109/02770900009055429>.
46. Kim JS, Tanaka N, Newell JD, et al. Nontuberculous mycobacterial infection: CT scan findings, genotype, and treatment responsiveness. *Chest* 2005; 128(6):3863–9. [https://doi.org/10.1016/S0012-3692\(15\)49628-X](https://doi.org/10.1016/S0012-3692(15)49628-X).
47. De Marca PGC, Goldenberg T, Mello FCQ, et al. Pulmonary densitovolumetry using computed tomography in patients with nontuberculous mycobacteria: correlation with pulmonary function tests. *Pulm Med* 2019;2019:e5942783. <https://doi.org/10.1155/2019/5942783>.
48. Lee Y, Song J-W, Chae EJ, et al. CT findings of pulmonary non-tuberculous mycobacterial infection in non-AIDS immunocompromised patients: a case-controlled comparison with immunocompetent patients. *Br J Radiol* 2013;86(1024):20120209. <https://doi.org/10.1259/bjr.20120209>.
49. Kennedy MP, Noone PG, Leigh MW, et al. High-resolution CT of patients with primary ciliary dyskinesia. *AJR Am J Roentgenol* 2007;188(5):1232–8. <https://doi.org/10.2214/AJR.06.0965>.
50. Kuo W, Soffers T, Andrinopoulou E-R, et al. Quantitative assessment of airway dimensions in young children with cystic fibrosis lung disease using chest computed tomography. *Pediatr Pulmonol* 2017; 52(11):1414–23. <https://doi.org/10.1002/ppul.23787>.
51. Bak SH, Kim S, Hong Y, et al. Quantitative computed tomography features and clinical manifestations associated with the extent of bronchiectasis in patients with moderate-to-severe COPD. *Int J Chron Obstruct Pulmon Dis* 2018;13:1421–31. <https://doi.org/10.2147/COPD.S157953>.